

Article

Functionalization of a Triazine Dendrimer Presenting Four Maleimides on the Periphery and a DOTA Group at the Core

Changsuk Lee, Kun Ji and Eric E. Simanek *

Department of Chemistry and Biochemistry, Texas Christian University, Fort Worth, TX 76129, USA; leecs73@hotmail.com (C.L.); kun.ji@tcu.edu (K.J.)

* Correspondence: e.simanek@tcu.edu; Tel.: +1-817-257-5355

Academic Editor: Ashok Kakkar

Received: 28 January 2016 ; Accepted: 26 February 2016 ; Published: 10 March 2016

Abstract: A readily and rapidly accessible triazine dendrimer was manipulated in four steps with 23% overall yield to give a construct displaying four maleimide groups and DOTA. The maleimide groups of the dendrimer are sensitive to hydrolysis under basic conditions. The addition of up to four molecules of water can be observed via mass spectrometry and HPLC. The evolution in the alkene region of the ¹H-NMR—the transformation of the maleimide singlet to the appearance of two doublets—is consistent with imide hydrolysis and not the Michael addition. The hydrolysis events that proceeded over hours are sufficiently slower than the desired thiol addition reactions that occur in minutes. The addition of thiols to maleimides can be accomplished in a variety of solvents. The thiols examined derived from cysteine and include the protected amino acid, a protected dipeptide, and native oligopeptides containing either 9 or 18 amino acids. The addition reactions were monitored with HPLC and mass spectrometry in most cases. Complete substitution was observed for small molecule reactants. The model peptides containing nine or eighteen amino acids provided a mixture of products averaging between 3 and 4 substitutions/dendrimer. The functionalization of the chelate group with gadolinium was also accomplished easily.

Keywords: dendrimer; triazine; DOTA; maleimide; peptide; bioconjugate; theranostic

1. Introduction

The term “theranostics” describes molecules that offer both therapeutic and diagnostic capabilities [1–6]. Theranostic small molecules include a reporting group—commonly a chelate for MRI or PET imaging—ligated to a pharmacophore. Theranostic nanoparticles elaborate this design with materials that can offer multivalent displays of the therapeutic and/or diagnostic agent(s), as well as leverage additional properties conveyed with size, including changes in biodistribution and targeting. Theranostic nanoparticles come in many varieties including magnetic [7], silica [8–10], gold/quantum dots [11–13], graphene [14], liposomal [15,16], and polymeric [17,18]. Dendritic materials offer a compelling platform in this area [19,20] given the opportunity to exquisitely control chemistry to manipulate any number of properties displayed across multiple nanoparticle classes, so-called nanoperiodicity [21–23], including size, ligand density and solubility. Versatility is a key criterion for the design of such targets. Here, we report on a tetravalent platform, **1** (Figure 1). Target **1** comprises three different domains: a reporter domain, a functional domain, and a dendritic domain. The reporter domain presents a DOTA group that can host metals for diagnostic applications such as PET or MRI. The functional domain presents four maleimides that can be readily reacted with thiols. The functional domain is linked to the reporter domain through the dendritic domain. Here, the dendritic domain is a small, generation-1 triazine dendron.

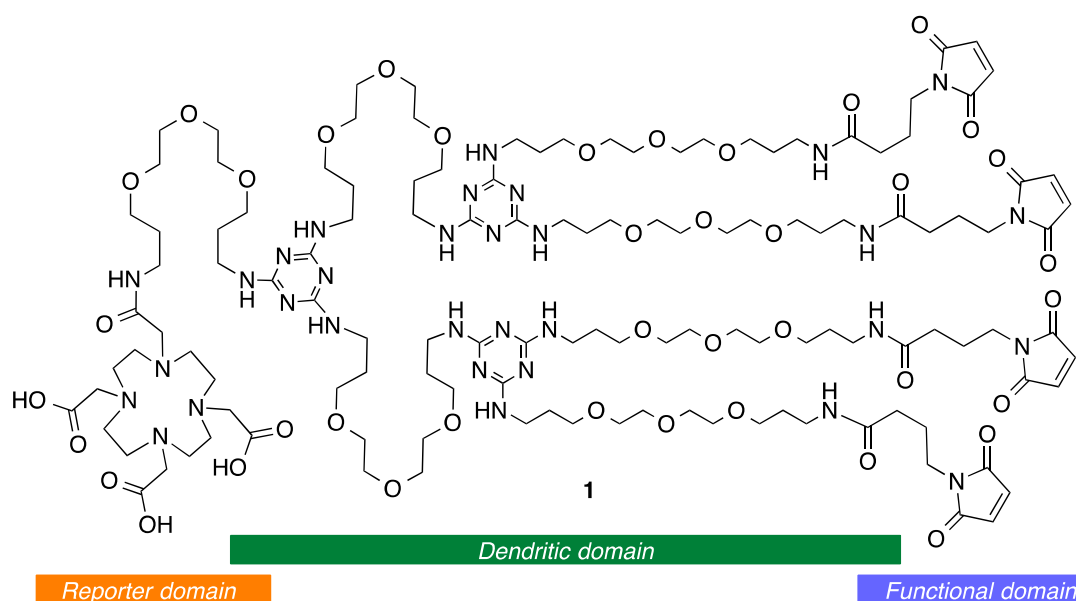


Figure 1. Target 1 with domains identified as reporter domain (orange), dendritic domain (green) and functional domain (blue).

2. Results and Discussion

2.1. Synthesis

The synthesis of **1** is shown in Scheme 1. It commences with the triazine dendron, **2**, which has been previously reported [24]. Intermediate **2** was obtained in less than 24 h using microwave-assisted reactions. The installation of the DOTA-reagent, **3**, was accomplished with HBTU to provide **4** in 43% yield. While mass spectrometry confirmed the structure of the product, the multiple conformations of the DOTA group led to broad signals in the $^1\text{H-NMR}$ spectra. The lines corresponding to the seven expected *tert*-butyl groups were well resolved, and integration matched expectation when compared with signature regions of the dendrimer.

To probe generality, and assess opportunities for potential future efforts that elaborate the dendritic portion in the presence of the reporter domain, we explored the feasibility of a two-step deprotection strategy. First, the Boc groups of **4** were selectively removed with a 1:1 mixture of 6 N HCl:MeOH to afford **5** in 79% isolated yield. Second, intermediate **5** was elaborated into a larger G3 dendrimer with 16 terminal groups (see Supplementary Materials). Then, intermediate **6** was obtained directly from **4** with a global deprotection step using a 1:1 mixture of TFA:CH₂Cl₂. Finally, the installation of the maleimides to produce **1** proceeded with 69% yield. This four-step synthetic sequence (starting from **4**) is executed with 23% overall yield. Gadolinium can be incorporated into **1** at this point (see Supplementary Materials).

2.2. Hydrolytic Stability

The hydrolytic stability of **1** in an aqueous solution is of significant concern: Commercially available maleimide crosslinking reagents are moisture sensitive, especially at pH > 7.5. To assess stability, **1** was added to slightly basic water (pH 7.5) and monitored by mass spectrometry and HPLC. After 4 h, the addition of up to four water molecules was clearly visible by both techniques. HPLC suggests that approximately 10% of **1** remains after 4 h under these slightly basic conditions. Under neutral conditions, however, the hydrolysis is much slower: Analysis of the $^1\text{H-NMR}$ suggests only 25% hydrolysis, observed after 2 days.

$^1\text{H-NMR}$ of the hydrolysis product is consistent with imide hydrolysis to a ring-opened, maleic acid amide. The alkene singlet of **1** appearing at 6.7 ppm is replaced with two doublets at 6.2 and

efficiency as determined by reaction times and product distributions. Since we predicted that **1** could serve as a building block for libraries, peptides **C** and **D** were used without extensive purification. Specifically, HPLC and MS analysis suggest that each peptide is present in greater than 60% in the crude cocktail obtained after precipitation of the cleavage product derived from a peptide synthesizer. To identify conjugates, the letter indicating the thiol and valency (when appropriate) is appended to the parent maleimide. That is, reaction of **7** and **A** produces **7-A₁** (or just **7-A**), whereas the product of three additions of **D** to **1** is identified as **1-D₃**.

A FmocCysOMe

C H₂N-CYGPPPPPG-COOH

B FmocCysTrpOMe

D H₂N-CGFQLRQPPLVSRKGEG-COOH

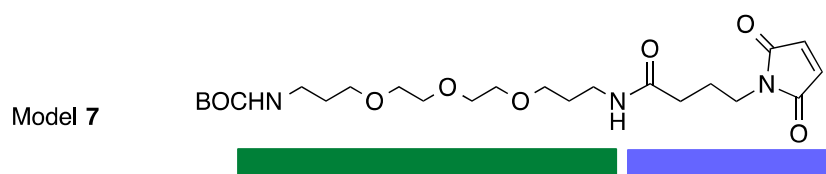


Figure 2. Thiols **A–D** in this study and model system **7** which models the dendritic domain (**green**) and functional domain (**blue**).

Compound **7** was prepared as a model to identify indicators of a successful reaction (Figure 2). The reactions of **7** with **A** (FmocCysOMe) and **B** (FmocCysTrpOMe) to yield conjugates **7-A** and **7-B**, respectively, were followed using NMR spectroscopy, mass spectrometry, and HPLC. Here, methylene chloride was used as a reaction solvent due to the limited water solubility of the protected amino acids. NMR spectroscopy provides convenient handles for assessing conjugation. The ¹H-NMR spectra showed a shift of the broad multiplet of the β-CH₂ of cysteine from ~3.0 ppm to 3.2 and 3.5 ppm with a pronounced diastereotopic splitting. Unfortunately, this region of the spectra was congested. The signals generated upon addition to the maleimide were more diagnostic. The methylene of the thioether appeared at 3.8 ppm. The adjacent methylene split into a diastereotopic pair at ~2.5 ppm (in an uncrowded region of the spectrum) and 3.1 ppm (in a more crowded region). The ¹³C-NMR was used to corroborate the addition. The appearance of diastereomers corresponding to the maleimide thioether (~39ppm), imide methylene (~36 ppm) and β-CH₂ of the cysteine residue (~34 ppm) were diagnostic for successful conjugation of the chiral thiol. The data from mass spectrometry and HPLC were consistent with a clean reaction between **7** and **A** or **B**. Mass spectrometry of the conjugates of **7-A** and **7-B** showed the parent ion with minor ions corresponding to the loss of both the Boc and Fmoc groups. Both **7-A** and **7-B** were isolated using column chromatography and obtained with approximately 60% yields. These low yields are attributed to the loss of Fmoc group during isolation.

Oxidation of the thiol offered the potential for a competing side-reaction. The cysteine disulfide of **A** appeared at 3.25 ppm in a crowded region of the ¹H-NMR spectrum. However, HPLC analysis provided a clear indication of this compound: The disulfides, thiols and conjugation products **7-A** and **7-B** showed unique retention times (See Supplementary Materials). Oxidation to the disulfide did not appear to be responsible for low yields of isolated materials. Accordingly, no special handling procedures were adopted for latter conjugation reactions.

Advantageously, we were able to perform conjugations with **1** in a range of solvents, because **1** was readily soluble in chloroform, dichloromethane, dioxane, methanol and water. For example, reactions of **1** with hydrophobic models **A** and **B** were performed in a dioxane:dichloromethane mixture. A dioxane:water mixture was used for nonapeptide **C**. For the hydrophilic peptide **D**, the conjugation was performed in water.

Conjugates **1-A₄** and **1-B₄** were isolated using chromatography with 65% and 54% yields. Mass spectrometry, and HPLC and NMR spectroscopy all provided corroborating data. HPLC showed that the retention times of thiol **A** and the conjugation product **1-A₄** were different by approximately

1 min. However, thiol **B** and the product of conjugation, **1-B₄**, showed similar retention times. The conjugation reaction using **A** and **B** were readily monitored by electrospray ionization-time of flight mass spectrometry, ESI-TOF MS (Figure 3a,b). Immediately upon mixing reagents, mass spectrometry showed clear evidence of conjugate formation with amino acid **A** reacting faster than dipeptide **B**.

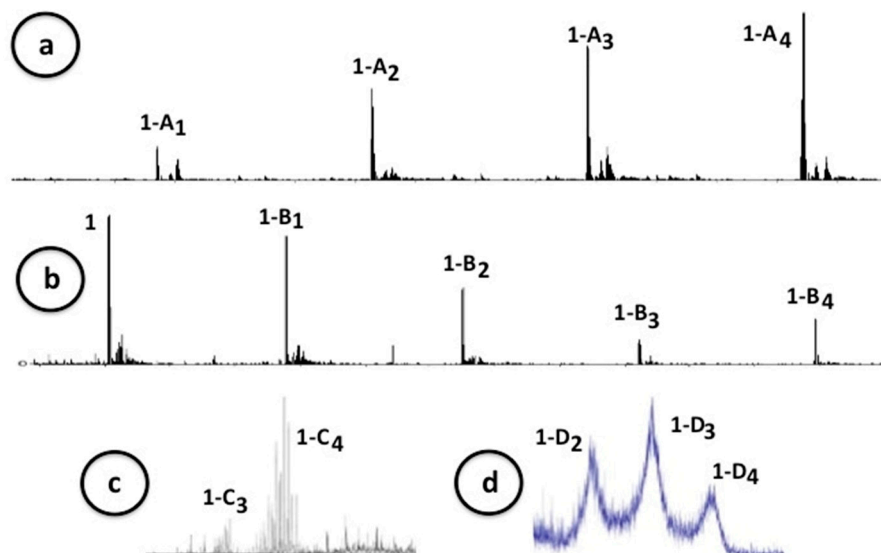


Figure 3. Conjugates **1** with **A** (a); **B** (b); **C** (c) and **D** (d). Traces (a,b) are taken upon the addition of thiol by ESI-TOF MS. Mass scales for these traces are m/z 2900–4400 (a) and m/z 2600–5200 (b); Traces (c,d) are taken of the purified product mixture. Mass scales for these traces are m/z 4500–7800 (c) and m/z 5000–13000 (d). Trace (d) was obtained by MALDI-TOF-MS.

2.4. Conjugation of Peptides

The products of conjugation of **1** with nonapeptide **C** were isolated in a multistep sequence. First, the reaction mixture was concentrated to an oil. The oil was then resuspended in deionized water to facilitate membrane filtration with a cellulose centrifugation filter (Ultracell YM3) with a 3 kDa molecular weight cutoff. After multiple rinses, the recovered volume was lyophilized to dryness. Using $^1\text{H-NMR}$, a comparison of the integration of the aromatic signals of the tyrosine with signals derived from the methylene, which was derived from the maleimide at 2.5 ppm (dendrimer), suggests that the product distribution approached the desired **1-C₄** target, approximately $\sim 1\text{-C}_{3.75}$. Mass spectrometry confirmed a successful reaction (Figure 3c). The presence of multiple lines at lower molecular weights than the target, **1-C₄**, is consistent with the use of an impure peptide.

Not surprisingly, these peaks were assignable (Figure 4). The desired product containing four copies of **C** is indicated with *four* green dots. Adducts of **1-C₄** with Na^+ and K^+ are shown with blue arrows. For lines corresponding to products with lower molecular weights, one or more of the peptides are missing amino acids. The most abundant ion displays a peptide missing a glycine residue (blue dot). Peptides missing proline (red dot) are also present. For simplicity, we indicate the minimum number of deletions for each peptide. That is, whether the final compound has one deletion in each peptide—or comprises three perfect peptides **C** and a peptide missing four amino acids—is unknown. The necessity of using double couplings during the solid phase synthesis of this proline-rich sequence is also reflected by the presence of a peak corresponding to a product with three copies of **C** and one copy of **C** containing an extra proline residue (purple circle). Given the distribution of products, it is unsurprising that the HPLC trace is broad.

The conjugation of 16-amino acid peptide, **D**, with **1** was followed using HPLC by monitoring the consumption of **1** and the appearance of new species. The reaction products were purified by membrane dialysis. MALDI-TOF mass spectrometry of the isolated product showed peaks

corresponding to **1-D₂**, **1-D₃**, and **1-D₄**. The broadness of the mass spectrum is consistent with both the use of impure peptides and the complications arising from salts of this highly charged peptide. The ¹H-NMR spectrum—albeit broad—showed neither maleimide nor maleic acid signals present in the reaction mixture as might be expected from the perceived low conversion rate. Although thiol addition should be faster than that the addition of any other functional group or solvent, steric congestion could retard this desired reaction and afford opportunities for intermolecular reaction of maleimides with amino acid side chains like that of lysine. The extent to which these reaction can occur as a function of lysine residue position will be assessed in a future study. Using ¹H-NMR, a comparison of peak areas derived from the aromatic phenylalanine peaks and methylene of maleimide suggests that the product distribution is centered at **1-D_{3,5}**, a more favorable ratio than what might be expected from casual inspection of the mass spectrum.

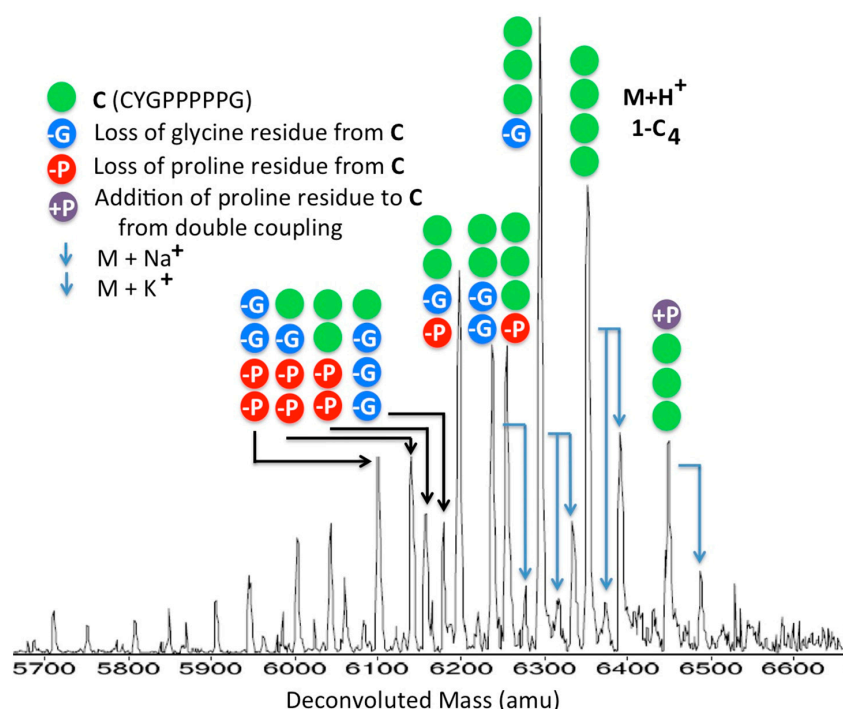


Figure 4. Tentative assignment of the products of conjugation of peptide C with **1** to yield **1-C₄**.

3. Experimental Section

3.1. General Synthetic Procedures

All chemicals were purchased from Aldrich (St. Louis, MO, USA) and Acros (Fair Lawn, NJ, USA) and used without further purification. All solvents were ACS grade and used without further purification. HPLC was carried out using an Agilent Technologies (Santa Clara, CA, USA) 1260 Infinity system and an Agilent Technologies 1260 Infinity DAD detector. NMR spectra were recorded on a Bruker Ascend 400 MHz spectrometer (Billerica, MA, USA) in CDCl₃, CD₃OD, or D₂O. All ESI mass spectral analyses were carried out by an Agilent Technologies 6224 TOF LC/MS system.

The chromatographic system used to measure sample purity consisted of a degasser (Agilent G1379B, Palo Alto, CA, USA), capillary pump (Agilent G1312B), micro well-plate auto sampler (Agilent G1367D), eclipse XDB-C18 column (4.6 mm i.d. × 150 mm, 5 μm, Agilent), and a diode array detector (Agilent G1316B). The mobile phase consisted of water/acetonitrile (A/B, HPLC grade, 0.1% (*w/v*) trifluoroacetic acid) at a flow rate of 0.8 mL/min. The elution gradient was 10% MeCN for 5 min, ramp to 90% MeCN in 30 min, and ramp down to 10% MeCN in 15 min. The sample volume injected 5 μL at a concentration 0.1 mg/mL with HPLC-grade MeCN, and detected at 214 nm.

3.2. Synthesis of Dendrimer 1

To a solution of **6** (31 mg, 0.014 mmol) and DIPEA (20 μ L, 0.115 mmol) in dioxane (1 mL), a solution of maleimide–NHS ester (32 mg, 0.115 mmol) in dichloromethane (1 mL) was added at RT then stirred for 48 h. The reaction was concentrated and purified by column chromatography (DCM:MeOH = 97:5 \rightarrow DCM:MeOH = 8:2) to give **1** (Figure 5) as a foam (28 mg, 69%). $^1\text{H-NMR}$ (400 MHz, CDCl_3): δ 6.71 (s, 8H), 3.64–3.32 (m, 120H, $\text{CH}_2\text{OCH}_2\text{CH}_2\text{OCH}_2\text{CH}_2\text{OCH}_2$, $\text{C}_3\text{N}_3\text{-NHCH}_2\text{CH}_2\text{CH}_2\text{O}$, DOTA- $\text{CONHCH}_2\text{CH}_2\text{CH}_2\text{O}$, $\text{CONHCH}_2\text{CH}_2\text{CH}_2\text{N}$, Maleimide- $\text{CONHCH}_2\text{CH}_2\text{CH}_2\text{O}$), 2.15 (t, $J = 7.2$, 8H), 1.92 (dt, $J = 14$, 7.2, 8H), 1.89–1.77 (br m, 28H, $\text{OCH}_2\text{CH}_2\text{CH}_2$); $^{13}\text{C-NMR}$ (100 MHz, CDCl_3) δ 171.7, 170.9, 134.1, 70.5 ($\text{OCH}_2\text{CH}_2\text{O}$), 70.2 ($\text{OCH}_2\text{CH}_2\text{O}$), 70.1 ($\text{OCH}_2\text{CH}_2\text{O}$), 69.8, 69.2 ($\text{CH}_2\text{CH}_2\text{CH}_2\text{O}$), 38.1 ($\text{NH}_2\text{CH}_2\text{CH}_2\text{CH}_2\text{O}$), 37.7 ($\text{CH}_2\text{CH}_2\text{CH}_2\text{O}$), 37.3 (maleimide), 33.6 (maleimide), 29.5 ($\text{NH}_2\text{CH}_2\text{CH}_2\text{CH}_2\text{O}$), 29.0 ($\text{NH}_2\text{CH}_2\text{CH}_2\text{CH}_2\text{O}$), 24.8 (maleimide); MS (ESI-TOF) calcd. for $\text{C}_{127}\text{H}_{214}\text{N}_{31}\text{O}_{40}$ 2813.5664, found 2813.5751 $[\text{M} + \text{H}]^+$. Spectra appear in the Supplementary Materials: Figures S1–S5.

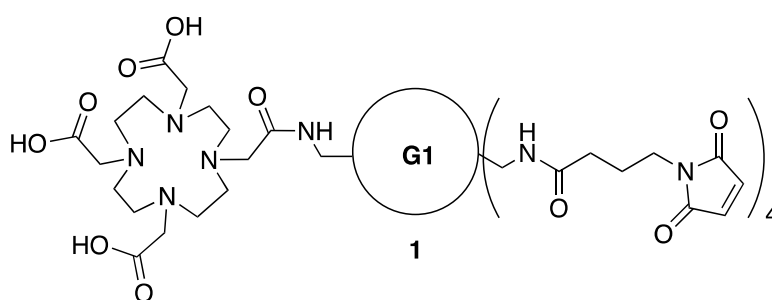


Figure 5. Intermediate 1.

3.3. Synthesis of Intermediate S1—Maleic Acid Amide of 1

A solution of **1** (8 mg) in water (1 mL) was adjusted to pH 7–8 with 1 N NaOH at RT then stirred for 18 h. The reaction mixture was lyophilized to give Intermediate **S1** (Figure 6). $^1\text{H-NMR}$ (400 MHz, D_2O): δ 6.23 (d, $J = 12.4$, 4H), 5.83 (d, $J = 12.4$, 4H), 3.55–3.12 (m, 120H, $\text{CH}_2\text{OCH}_2\text{CH}_2\text{OCH}_2\text{CH}_2\text{OCH}_2$, $\text{C}_3\text{N}_3\text{-NHCH}_2\text{CH}_2\text{CH}_2\text{O}$, DOTA- $\text{CONHCH}_2\text{CH}_2\text{CH}_2\text{O}$, $\text{CONHCH}_2\text{CH}_2\text{CH}_2\text{N}$, Maleimide- $\text{CONHCH}_2\text{CH}_2\text{CH}_2\text{O}$), 2.18 (t, $J = 7.4$, 8H), 1.89–1.77 (br m, 36H, $\text{OCH}_2\text{CH}_2\text{CH}_2$, Maleimide); $^{13}\text{C-NMR}$ (100 MHz, D_2O) δ 180.0 (DOTA-acid), 179.9 (DOTA-acid), 175.7 (Maleimide- $\text{CONHCH}_2\text{CH}_2\text{CH}_2\text{O}$), 174.3 (DOTA-amide), 173.2 (DOTA-acid), 168.1 (conjugate amide), 165.3 (triazine, conjugate acid), 135.7, 124.9, 69.7, 69.6, 69.5, 69.4, 68.6, 68.4, 38.5, 37.4, 37.3, 36.4, 33.1, 28.9, 28.3, 24.9 (maleimide); MS (ESI-TOF) calcd. for $\text{C}_{127}\text{H}_{222}\text{N}_{31}\text{O}_{44}$ 2885.6087, found 2885.6806 $[\text{M} + \text{H}]^+$. Spectra appear in the Supplementary Materials: Figures S6–S9.

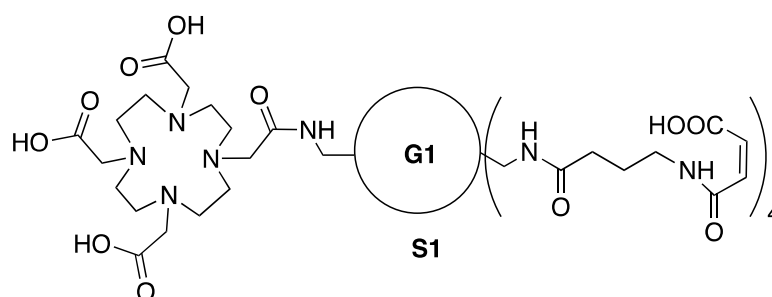


Figure 6. Intermediate S1.

3.4. Synthesis of Intermediate 4

To a solution of **2** (194 mg, 0.09 mmol) and **3** (52 mg, 0.09 mmol) in acetonitrile (8 mL), HBTU (34 mg, 0.09 mmol) was added followed by triethylamine (25 μ L, 0.18 mmol) at RT. The reaction

was stirred for 18 h. The reaction was diluted with 30 mL dichloromethane and washed 0.1 N HCl (30 mL), 10% NaHCO₃ (30 mL), brine (30 mL), then dried over MgSO₄, and concentrated. The crude product was purified by column chromatography (DCM:MeOH = 97:5 → DCM:MeOH = 85:15) to give **4** (Figure 7) as a foam (105 mg, 43%). ¹H-NMR (400 MHz, CDCl₃): δ 3.68–3.47 (m, 104H, CH₂OCH₂CH₂OCH₂CH₂OCH₂, C₃N₃-NHCH₂CH₂CH₂O, DOTA-CONHCH₂CH₂CH₂O), 3.22–3.18 (br m, 8H, BocNHCH₂), 1.84–1.72 (m, 28H, OCH₂CH₂CH₂), 1.46 (s, 9H), 1.45 (s, 9H), 1.42 (s, 45H); ¹³C-NMR (100 MHz, CDCl₃) δ 176.6 (DOTA-OCO^tBu), 174.4 (DOTA-OCO^tBu), 172.3 (DOTA-OCO^tBu), not found (C₃N₃), 156.0 (NHCO^tBu), 81.7 (DOTA-OC(CH₃)₃), 78.7 (C(CH₃)₃), 70.47 (OCH₂CH₂O), 70.21 (OCH₂CH₂O), 70.17 (OCH₂CH₂O), 70.10 (OCH₂CH₂O), 69.42 (CH₂CH₂CH₂O), 69.02 (CH₂CH₂CH₂O), 57.5 (DOTA), 56.2 (DOTA), 55.6 (DOTA), 53.5 (DOTA), 41.9 (NH₂CH₂CH₂CH₂O), 38.5 (CH₂CH₂CH₂O), 38.4 (CH₂CH₂CH₂O), 29.6 (NH₂CH₂CH₂CH₂O), 29.3 (NH₂CH₂CH₂CH₂O), 28.4 (C(CH₃)₃), 27.94 (DOTA-OC(CH₃)₃), 27.87 (DOTA-OC(CH₃)₃); MS (ESI-TOF) calcd. for C₁₂₇H₂₄₂N₂₇O₃₆ 2721.7936, found 2721.8117 [M + H]⁺. Spectra appear in the Supplementary Materials: Figures S11–S13.

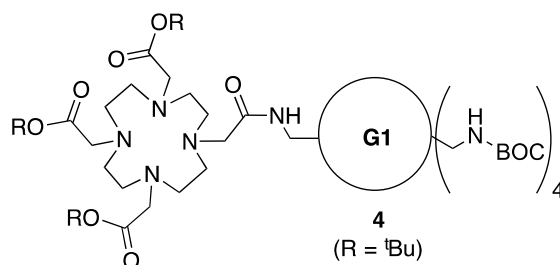


Figure 7. Intermediate 4.

3.5. Synthesis of Intermediate 5

To a solution of **4** (59 mg, 0.022 mmol) in methanol (2 mL), 6 N HCl (aq) (2 mL) was added at RT then stirred for 8 h. The reaction was diluted with ethyl acetate (10 mL) and water (2 mL). Water layer was basifying with 5 N NaOH (aq) then the desired compound was extracted with dichloromethane (10 mL × 8). Combined organic layers was dried over MgSO₄, and concentrated to give **5** (40.5 mg of as a clear oil; Figure 8). ¹H-NMR (400 MHz, CDCl₃): δ 3.63–3.42 (m, 104H, CH₂OCH₂CH₂OCH₂CH₂OCH₂, C₃N₃-NHCH₂CH₂CH₂O, DOTA-CONHCH₂CH₂CH₂O), 3.10 (br s, 8H, NH₂CH₂), 1.96–1.82 (br m, 28H, OCH₂CH₂CH₂), 1.45 (s, 27H); ¹³C-NMR (100 MHz, CDCl₃) δ 172.5 (DOTA-OCO^tBu), 171.5 (DOTA-OCO^tBu), 165.8 (C₃N₃), 81.8 (DOTA-OC(CH₃)₃), 81.7 (DOTA-OC(CH₃)₃), 70.54 (OCH₂CH₂O), 70.42 (OCH₂CH₂O), 70.19 (OCH₂CH₂O), 70.11 (OCH₂CH₂O), 69.95 (OCH₂CH₂O), 69.40 (CH₂CH₂CH₂O), 69.27 (CH₂CH₂CH₂O), 56.1 (Dota), 55.7 (Dota), 55.6 (DOTA), 39.0 (NH₂CH₂CH₂CH₂O), 38.1 (CH₂CH₂CH₂O), 29.7 (NH₂CH₂CH₂CH₂O), 29.5 (NH₂CH₂CH₂CH₂O), 29.1 (NH₂CH₂CH₂CH₂O), 28.10 (DOTA-OC(CH₃)₃), 27.98 (DOTA-OC(CH₃)₃); MS (ESI-TOF) calcd for C₁₀₇H₂₁₀N₂₇O₂₈ 2321.5839, found 2321.6677 [M + H]⁺. Spectra appear in the Supplementary Materials: Figures S14–S16.

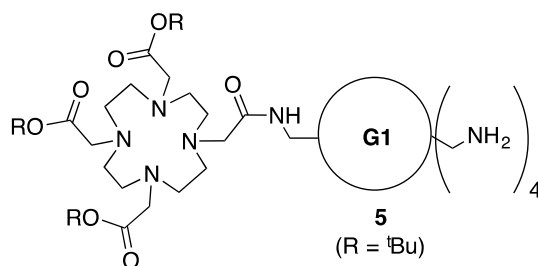


Figure 8. Intermediate 5.

3.6. Synthesis of Intermediate—Generation 3 Dendrimer with DOTA

A solution of **5** (79 mg, 0.034 mmol) and **M** (Macromonomer [24]) (542 mg, 0.27), and DIPEA (71 mL, 0.41 mmol) in THF (3 mL), dioxane (1 mL), *i*-propanol (70%) (0.5 mL) was stirred at 75 °C in a capped vessel for 4 d. The solution was evaporated under vacuum. The residue was dissolved in dichloromethane, washed with brine, dried over MgSO₄, and concentrated. The crude product was purified by column chromatography. The crude product was purified by column chromatography (DCM:MeOH = 97:5 → DCM:MeOH = 85:15) to give **S3** (Figure 9) as a foam (92 mg, 27%). ¹H-NMR (400 MHz, CDCl₃): δ 3.65–3.42 (m, 464H, CH₂OCH₂CH₂OCH₂CH₂OCH₂, C₃N₃-NHCH₂CH₂CH₂O, DOTA-CONHCH₂CH₂CH₂O), 3.22–3.19 (br m, 32H, BocNHCH₂), 1.81–1.72 (br m, 124H, OCH₂CH₂CH₂), 1.47 (s, 9H), 1.45 (s, 9H), 1.44 (s, 9H), 1.42 (s, 144H); ¹³C-NMR (100 MHz, CDCl₃) δ not found (DOTA-OCO^tBu), not found (DOTA-OCO^tBu), not found (DOTA-OCO^tBu), not found (C₃N₃), 156.1 (NHCO^tBu), 81.85 (DOTA-OC(CH₃)₃), 81.79 (DOTA-OC(CH₃)₃), 78.8 (C(CH₃)₃), 70.56 (OCH₂CH₂O), 70.28 (OCH₂CH₂O), 70.23 (OCH₂CH₂O), 70.19 (OCH₂CH₂O), 69.52 (CH₂CH₂CH₂O), 69.22 (CH₂CH₂CH₂O), 69.17 (CH₂CH₂CH₂O), not found (DOTA), not found (DOTA), not found (DOTA), 53.4 (DOTA), 41.8 (NH₂CH₂CH₂CH₂O), 38.5 (CH₂CH₂CH₂O), 38.2 (CH₂CH₂CH₂O), 29.67 (NH₂CH₂CH₂CH₂O), 29.60 (NH₂CH₂CH₂CH₂O), 29.54 (NH₂CH₂CH₂CH₂O), 29.33 (NH₂CH₂CH₂CH₂O), 28.5 (C(CH₃)₃), 28.01 (DOTA-OC(CH₃)₃), 27.94 (Dota-OC(CH₃)₃); MS (ESI-TOF) calcd for C₄₆₃H₈₇₈N₁₁₁O₁₃₂ 10106.5403, found 10114.2078 [M + H]⁺. Spectra appear in the Supplementary Materials: Figures S17–S19.

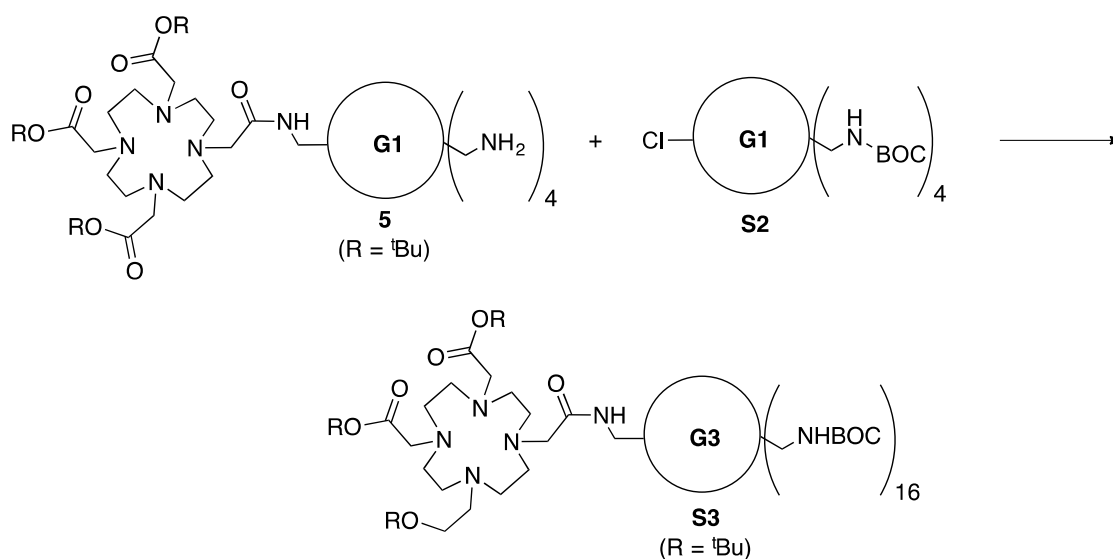


Figure 9. Synthesis of Intermediate **S3**.

3.7. Synthesis of Intermediate **6**

To a solution of **5** (68 mg, 0.029 mmol) in dichloromethane (2 mL), trifluoroacetic acid (2 mL) was added at RT then stirred for 20 h. Subsequently the reaction mixture was evaporated under vacuum. The residue was decanted with diethyl ether (5 mL × 3), and dried under vacuum to give **6** (Figure 10) as a white powder (quantitative). ¹H-NMR (400 MHz, CD₃OD): δ 3.55–3.26 (m, 104H, CH₂OCH₂CH₂OCH₂CH₂OCH₂, C₃N₃-NHCH₂CH₂CH₂O, DOTA-CONHCH₂CH₂CH₂O), 2.99 (br t, J = 6.2, 8H, NH₂CH₂), 1.85–1.76 (br m, 28H, OCH₂CH₂CH₂); ¹³C-NMR (100 MHz, CD₃OD) δ 164.8, 157.4 156.4, 71.6, 71.53, 71.50, 71.33, 71.23, 71.21, 70.23, 69.91, 69.76, 69.73, 39.87, 39.64, 39.44, 39.35, 39.27, 39.19, 38.09, 38.03, 30.86, 30.45, 30.35, 30.19, 30.12; MS (ESI-TOF) calcd. for C₉₅H₁₈₆N₂₇O₂₈ 2153.3961, found 2153.4295 [M + H]⁺. Spectra appear in the Supplementary Materials: Figures S20–S22.

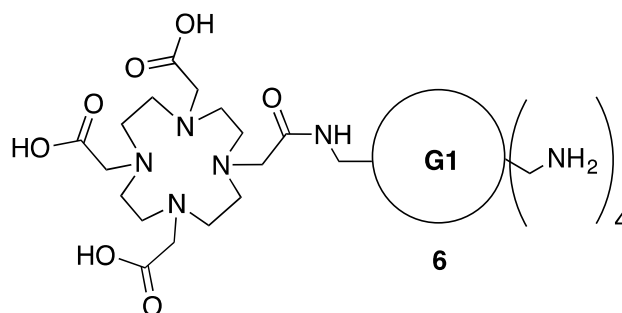


Figure 10. Intermediate 6.

3.8. Synthesis of Model 7

To a solution of commercially-available maleimide succinimide ester **S5** (17 mg, 0.06 mmol) in dichloromethane (3.0 mL), a solution of monoBoc amine **S4** (16 mg, 0.05 mmol) in dichloromethane (1.0 mL) was added at RT. The solution was stirred for 3h at RT and evaporated under vacuum. The crude product was purified by column chromatography (DCM:MeOH = 99:1 → DCM:MeOH = 97:3) to give **7** (Figure 11) as a solid (21 mg, 86%). ¹H-NMR (400 MHz, CDCl₃): δ 6.71 (s, 2H, n), 3.67–3.53 (m, 14H, c, d, e, f, g, h, m), 3.36 (q, *J* = 6.4, 2H, j), 3.23 (q, *J* = 6.4, 2H, a), 2.16 (t, *J* = 6.4, 2H, k), 1.97–1.94 (m, 2H, l), 1.82–1.75 (m, 4H, b, i), 1.43 (s, 9H, Boc) ¹³C-NMR (100 MHz, CDCl₃) δ 171.6, 170.8, 156.0, 134.1, 78.9, 70.5, 70.4, 70.2, 70.1, 69.8, 69.5, 38.4, 37.8, 37.2, 33.6, 29.6, 28.9, 28.4, 24.7; MS (ESI-TOF) calcd. for C₂₃H₄₀N₃O₈ 486.2815, found 486.4100 [M + H]⁺. Spectra appear in the Supplementary Materials: Figures S23–S25.

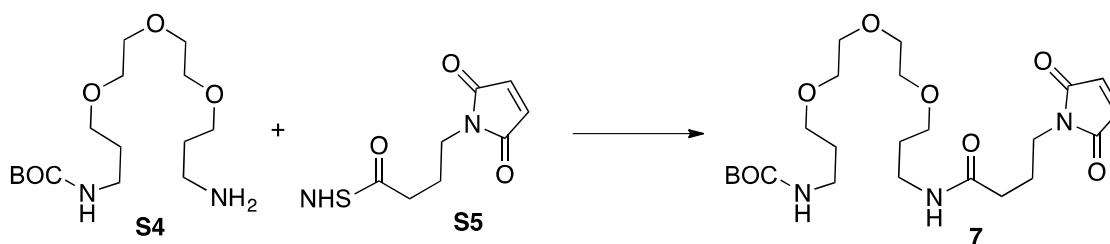


Figure 11. Synthesis of 7.

3.9. Synthesis of Conjugate 7-A

To a solution of **1** (35 mg, 0.07 mmol) in dioxane (1.0 mL) a solution of cysteine **A** (28 mg, 0.079) in dichloromethane (1.0 mL) was added at RT. The solution was stirred for 48h at room temperature and evaporated under vacuum. The crude product was purified by column chromatography (DCM = 100 → DCM:MeOH = 95:5) to give **7-A** (Figure 12) as a oil (37 mg, 61%). ¹H-NMR (400 MHz, CDCl₃): δ 7.76 (d, *J* = 8.0, 2H, FMOC), 7.61 (t, *J* = 6.0, 2H, FMOC), 7.42–7.28 (m, 4H, FMOC), 5.00 (br s, 1H, NH), 4.71–4.68 (m, 1H, p), 4.49–4.41 (m, 2H, FMOC), 4.24 (t, *J* = 6.8, 1H, FMOC), 3.83–3.75 (m, 1H, n), 3.80 (s, 3H, q), 3.65–3.51 (m, 14H, c, d, e, f, g, h, m), 3.46 (dd, *J* = 14, 6.0, 1H, o), 3.37–3.31 (m, 2H, j), 3.23–3.19 (m, 2H, a), 3.15–3.03 (m, 2H, n'), 2.50–2.39 (m, 1H, n'), 2.15 (t, *J* = 7.2, 2H, k), 1.99–1.90 (m, 2H, l), 1.80–1.75 (m, 4H, b, i), 1.43 (s, 9H, Boc) ¹³C-NMR (100 MHz, CDCl₃) δ 176.7, 174.5, 174.3, 171.5 (ester), 170.9 (amide), 156.0 (Boc), 155.9 (FMOC), 143.8, 143.7, 143.6, 141.3, 127.7, 127.1, 127.0, 125.1, 125.0, 119.98, 119.94, 70.4, 70.1, 70.0, 69.7, 69.4, 67.1, 52.9, 52.8, 47.1, 39.6, 38.6, 38.5, 38.4, 37.7, 36.0, 35.6, 33.5, 33.4, 29.6, 28.9, 28.4, 23.6, 23.55; MS (ESI-TOF) calcd. for C₄₂H₅₉N₄O₁₂S 843.3850, found 843.5872 [M + H]⁺. Spectra appear in the Supplementary Materials: Figures S26–S28.

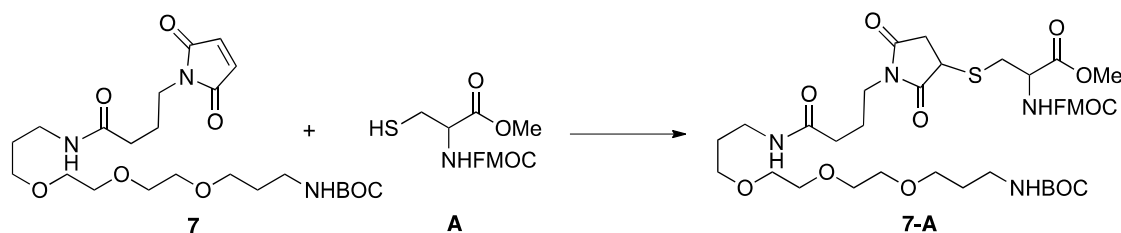


Figure 12. Synthesis of 7-A.

3.10. Synthesis of Cystine (S6)

To a solution of **A** (59 mg, 0.165 mmol) in dichloromethane (4.0 mL), solid iodine (10 mg, 0.082 mmol) was added at RT. The solution was stirred for 2 h at room temperature and evaporated under vacuum. The crude product was purified by column chromatography (Ethyl Acetate: Hexanes = 1:9 → Ethyl Acetate: Hexanes = 3:7) to give **S6** (Figure 13) as white powder (46 mg, 39%). ¹H-NMR (400 MHz, CDCl₃): δ 7.74 (d, *J* = 7.2, 2H, FMOC), 7.59–7.57 (br s, 2H, FMOC), 7.39–7.27 (m, 4H, FMOC), 5.77 (br d, *J* = 7, 1H, NH), 4.70–4.65 (m, 1H), 4.4–4.39 (m, 2H, FMOC), 4.20 (t, *J* = 7.0, 1H, FMOC), 3.74 (s, 3H), 3.17 (d, *J* = 4.8, 2H); ¹³C-NMR (100 MHz, CDCl₃) δ 170.9, 155.7, 143.8, 143.7, 141.3, 127.8, 127.1, 125.1, 120.0, 67.3, 53.3, 52.9, 47.1, 41.1; MS (ESI-TOF) calcd. for C₃₈H₃₇N₂O₈S₂ 713.83898, found 713.3859 [M + H]⁺. Spectra appear in the Supplementary Materials: Figures S29–S34.

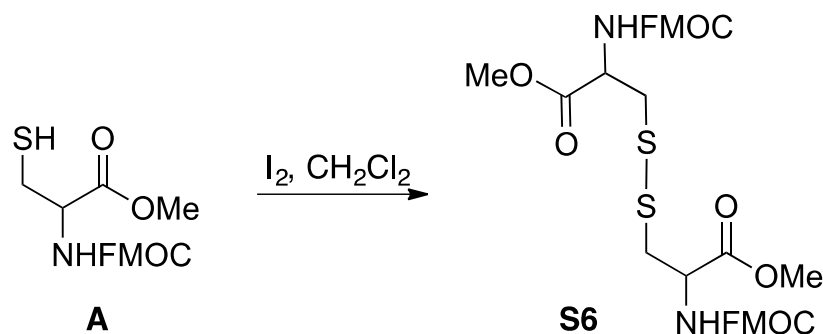


Figure 13. Synthesis of S6.

3.11. Synthesis of Conjugate 7-B

To a solution of **7** (12 mg, 0.025 mmol) in dioxane (1.0 mL), a solution of **B** (18 mg, 0.033) in dichloromethane (1.0 mL) was added at RT. The solution was stirred for 48 h at room temperature and evaporated under vacuum. The crude product was purified by column chromatography (DCM = 100 → DCM:MeOH = 95:3) to give **7-B** (Figure 14) as an oil (16.5 mg, 64%). ¹H-NMR (400 MHz, CDCl₃): δ 7.75 (t, *J* = 7.6, 2H), 7.58 (d, *J* = 7.1, 2H), 7.52 (t, *J* = 8.5, 1H), 7.42–7.25 (m, 6H), 7.14–7.03 (m, 2H), 4.98–4.84 (m, 2H), 4.69–4.44 (m, 1H), 4.44–4.34 (m, 2H), 4.23–4.17 (m, 1H), 4.04 (br s, 1H), 3.59–3.45 (m, 18H), 3.40–2.80 (m, 9H), 2.47–2.41 (m, 1H), 2.23–2.17 (m, 2H), 2.00–1.86 (m, 2H), 1.79–1.75 (m, 4H), 1.43 (s, 9H) ¹³C-NMR (100 MHz, CDCl₃) δ 178.1, 177.5, 174.6, 174.4, 172.1, 172.0, 171.9, 169.7, 169.6, 156.1, 143.8, 143.7, 141.3, 136.6, 136.4, 127.8, 127.4, 127.3, 127.1, 125.1, 124.1, 121.8, 121.7, 120.0, 119.96, 119.91, 119.2, 119.1, 118.4, 118.3, 111.5, 108.6, 108.2, 79.0, 70.5, 70.2, 70.1, 69.8, 69.4, 67.2, 67.0, 53.4, 52.9, 52.7, 52.5, 52.4, 47.1, 47.06, 40.8, 39.4, 38.8, 38.4, 38.2, 37.9, 36.7, 35.9, 33.3, 33.2, 28.5, 27.4, 23.4, 23.3; MS (ESI-TOF) calcd for C₅₃H₆₉N₆O₁₃S 1029.4643, found 1029.6996 [M + H]⁺. Spectra appear in the Supplementary Materials: Figures S35–S38.

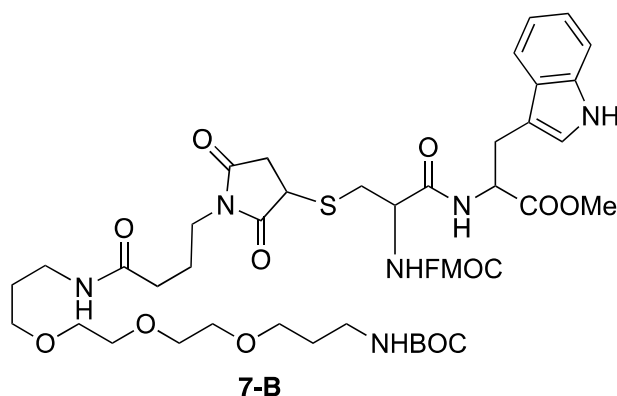
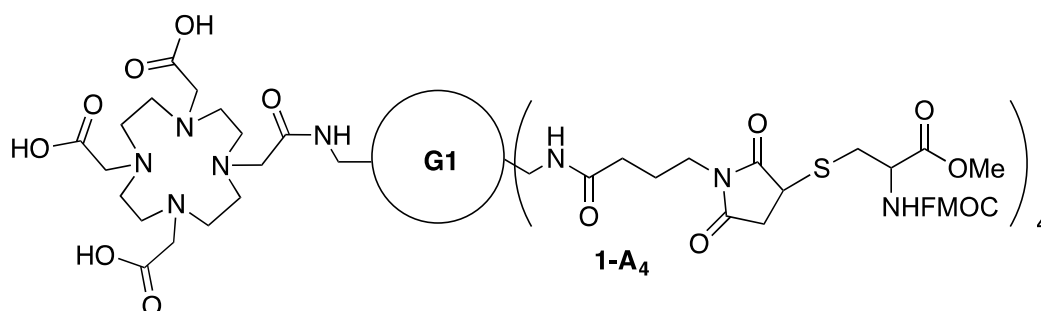


Figure 14. Intermediate 7-B.

3.12. Synthesis of Conjugate 1-A₄

To a solution of **1** (26 mg, 0.009 mmol) in dioxane (1.0 mL) a solution of **A** (25 mg, 0.074) in dichloromethane (1.0 mL) was added at RT. The solution was stirred for 48 h at room temperature and evaporated under vacuum. The crude product was purified by column chromatography (DCM = 100 → DCM:MeOH = 9:1) to give **1-A₄** (Figure 15) as an oil (25 mg, 65%). ¹H-NMR (400 MHz, CDCl₃): δ 7.75 (d, *J* = 7.5, 8H, FMOC), 7.61 (t, *J* = 7.2, 8H, FMOC), 7.41–7.29 (m, 16H, FMOC), 4.68 (br s, 4H, p), 4.44–4.40 (m, 8H, FMOC), 4.23 (t, *J* = 7.2, 4H, FMOC), 3.81–3.70 (m, 4H, n), 3.78 (s, 3H, OCH₃), 3.69–3.10 (m, 128H, a, c, d, e, f, g, h, j, m, n', o), 2.48–2.38 (m, 4H, n'), 2.14 (t, *J* = 6.5, 8H, k), 1.94–1.65 (m, 36H, b, i, l); ¹³C-NMR (100 MHz, CDCl₃) δ 177.0, 176.7, 174.6, 174.4, 171.7, 171.0, 156.0, 143.8, 143.7, 141.3, 127.8, 127.1, 125.2, 11.98, 70.55, 70.46, 70.2, 70.0, 69.7, 69.2, 67.1, 54.2, 53.3, 52.9, 52.8, 47.1, 39.7, 38.7, 38.6, 38.2, 37.7, 36.1, 35.7, 34.4, 33.1, 33.52, 33.46, 29.6, 29.3, 29.0, 23.7, 23.6; MS (ESI-TOF) calcd. for C₂₀₃H₂₉₀N₃₅O₅₆S₄ 4241.9804, found 4243.7824 [M + H]⁺. Spectra appear in the Supplementary Materials: Figures S39–S44.

Figure 15. Dendrimers 1-A₄.

3.13. Synthesis of Conjugate 1-B₄

To a solution of **1** (11 mg, 0.0025 mmol) in dioxane (1.0 mL) a solution of **B** (17 mg, 0.031 mmol) in dichloromethane (1.0 mL) was added at RT. The solution was stirred for 48h at room temperature and evaporated under vacuum. The crude product was purified by column chromatography (DCM = 100 → DCM:MeOH = 9:1) to give **1-B₄** (Figure 16) as an oil (10.5 mg, 54%). ¹H-NMR (400 MHz, CDCl₃): δ 7.75–7.00 (m, 52H), 4.89–4.01 (m, 20H, p, q, FMOC), 3.46–2.95 (m, 152H, a, c, d, e, f, g, h, j, m, n, o, r, OMe), 2.88–2.81 (m, 4H, n'), 2.37–2.31 (m, 4H, n'), 2.28–2.17 (m, 8H, k), 1.97–1.59 (m, 36H, b, i, l); ¹³C-NMR (100 MHz, CDCl₃) δ 177.9, 177.5, 174.6, 174.5, 172.0, 172.0, 169.9, 156.2, 143.8, 143.7, 141.3, 136.6, 136.4, 127.8, 127.4, 127.1, 125.2, 124.1, 121.6, 120.0, 119.94, 119.1, 118.3, 118.2, 111.6, 108.6, 108.3, 70.4, 70.1, 70.0, 69.8, 69.6, 69.1, 67.2, 67.1, 55.1, 53.5, 53.3, 53.0, 52.8, 52.43, 52.38, 47.1, 40.6, 39.4, 38.7, 38.1, 37.9, 37.7, 36.3, 35.9, 33.3, 33.2, 29.7, 29.3, 29.0, 27.4, 23.5, 22.7; MS (ESI-TOF) calcd.

for $C_{247}H_{330}N_{42}O_{60}S_4$ 4986.2976, found 4989.1225 $[M + H]^+$. Spectra appear in the Supplementary Materials: Figures S45–S49.

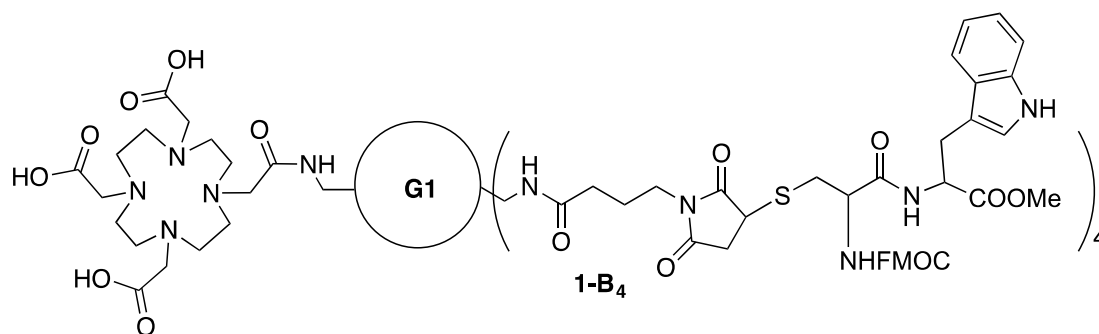


Figure 16. Dendrimer 1-B₄.

3.14. Synthesis of Conjugate 1-C₄

To a solution of maleimide **1** (9.8 mg, 0.0034 mmol) in dioxane (0.5 mL), a solution of CYGPPPPPG **C** (25 mg, 0.0279 mmol) in water (0.5 mL) was added, followed by addition of DIPEA (10 μ L, 0.056 mmol) at RT. The solution was stirred for 18h at room temperature and then evaporated under vacuum. The crude product was diluted with deionized water (1.5 mL) and excess amount of peptide was removed from the dendron by centrifugal filtration (3000 MW cut off, 4000 rpm). The residue was washed with deionized water (2 mL) five times and lyophilized to give **1-C₄** (Figure 17) as a solid (14 mg, 63%). ¹H-NMR (400 MHz, D₂O): δ 7.19–7.06 (m, 8H, x), 6.89–6.73 (m, 8H, y), 4.64–4.57 (m, 20H, t), 4.37–4.34 (m, 4H, q), 4.26–4.22 (m, 4H, p), 3.99–3.86 (m, 8H, s), 3.85–3.68 (m, 32H, n, s, w), 3.65–2.81 (m, 156H, a, c, d, e, f, g, h, m, n', o, r, w), 2.59–2.51 (m, 4H, n'), 2.31–2.15 (m, 28H, k, u), 2.05–1.65 (m, 96H, b, i, l, u, v); ¹³C-NMR (100 MHz, D₂O) δ 178.8, 178.7, 176.8, 174.8, 174.7, 174.1, 173.2, 173.1, 171.7, 171.4, 170.85, 170.7, 169.1, 167.1, 166.9, 162.2, 161.9, 154.0, 153.9, 129.8, 129.75, 127.0, 126.8, 117.0, 114.6, 114.1, 71.3, 68.9, 68.65, 67.8, 67.6, 67.5, 65.8, 61.7, 60.2, 59.7, 58.5, 57.8, 55.7, 55.0, 54.7, 54.6, 51.7, 50.9, 50.0, 47.5, 47.4, 46.9, 46.8, 46.2, 42.0, 41.9, 40.8, 37.8, 37.0, 35.7, 35.4, 34.8, 32.1, 28.5, 27.6, 27.3, 27.1, 23.9, 23.5, 22.2; MS (ESI-TOF) calcd. for $C_{291}H_{442}N_{67}O_{84}S_4$ 6347.1257, found 6295.1574 $[M + H]^+$. Spectra appear in the Supplementary Materials: Figures S50–S55.

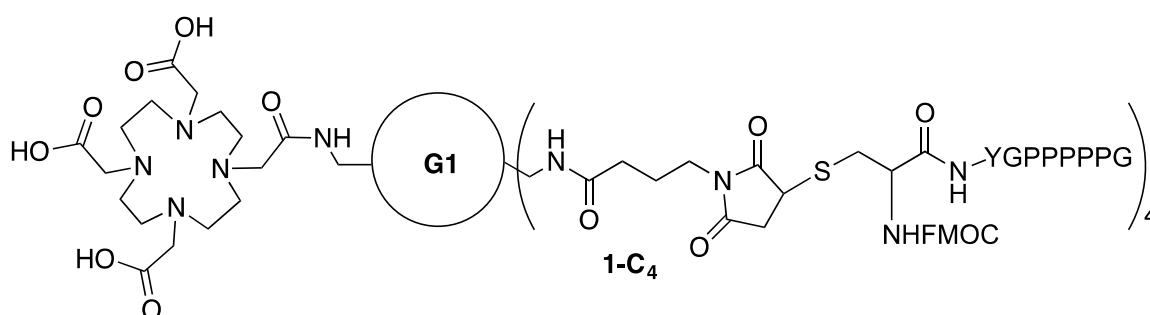


Figure 17. Dendrimer 1-C₄.

3.15. Synthesis of Conjugate 1-D₄

To a solution of **1** (9.1 mg, 0.0032 mmol) in water (0.5 mL), a solution of CGFQLRQPPLVPSRKGE, **D** (51 mg, 0.026 mmol) in water (0.5 mL) was added followed by addition of 0.1 N NaOH (adjust pH ~ 7–8). The solution was stirred for 18 h at RT before diluting with deionized water (1.0 mL). Excess peptide was removed by centrifugal filtration (3000 MW cut off, 4000 rpm). The residue was washed with deionized water (2 mL) five times and lyophilized to give **1-D₄** (Figure 18) as a solid (19.7 mg,

57%). $^1\text{H-NMR}$ (400 MHz, D_2O): δ 7.25–7.13 (m, 20H, 2), 4.61–4.49 (m, 8H, r, x), 4.39–4.22 (m, 52H, p, s(2), t(2), u(2), v(3), w, y, z), 3.95–2.90 (m, 224H, a, c, d, e, f, g, h, j, m, n, n', o, q(3), 1, 10(2), 11(3), 16, 20), 2.58–2.52 (m, 4H, n'), 2.33–2.13 (m, 44H, k, 4(2), 13(3), 22), 2.13–1.34 (m, 168H, b, i, l, 3(2), 5(2), 6(2), 8(2), 9(2), 12(3), 13(3), 14, 17, 18, 19, 21), 0.92–0.78 (m, 72H, 7(2), 15) $^{13}\text{C-NMR}$ (100 MHz, D_2O) δ 181.0, 179.4, 179.2, 177.7, 176.2, 174.8, 174.3, 174.1, 173.8, 173.3, 173.2, 173.0, 172.4, 171.8, 171.6, 171.2, 170.7, 170.4, 169.8, 156.7, 136.1, 129.2, 128.7, 127.2, 69.7, 69.4, 68.5, 68.4, 61.0, 60.5, 60.0, 58.8, 56.8, 56.4, 55.8, 55.5, 55.0, 53.9, 53.5, 53.2, 53.0, 52.7, 52.5, 50.8, 48.3, 47.9, 47.7, 43.5, 42.5, 40.5, 39.7, 39.1, 38.5, 37.7, 37.1, 36.5, 33.4, 32.9, 31.0, 30.7, 30.2, 30.1, 29.5, 29.3, 28.6, 28.4, 28.2, 27.8, 27.0, 26.2, 24.7, 24.4, 23.0, 22.2, 22.0, 21.9, 21.1, 21.0, 18.3, 17.6; MS (MALDI-TOF) calcd. for $\text{C}_{471}\text{H}_{777}\text{N}_{139}\text{O}_{136}\text{S}_4$ 10684., found 10662. Spectra appear in the Supplementary Materials: Figures S56–S60.

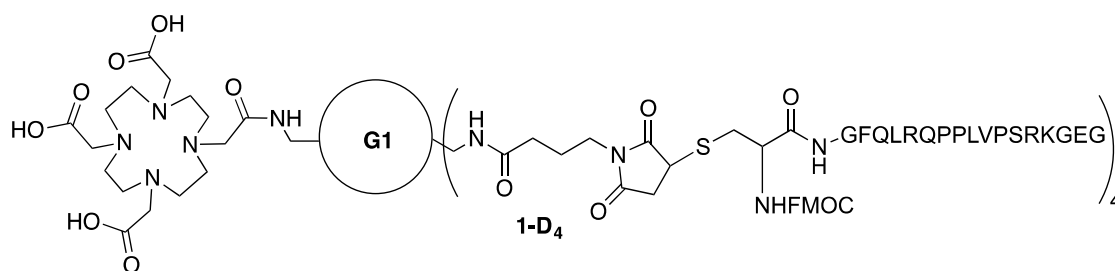


Figure 18. Dendrimer 1-D₄.

4. Conclusions

In conclusion, **1** represents a valuable platform for the pursuit of theranostic applications. Mass spectrometry provides evidence that, upon metallation with gadolinium, **1-Gd** can be reacted with **A** to yield **1-A₄-Gd**. This construct and related conjugates will be described in due course. While poly(maleimides) are commercially available (Toronto Research Chemicals), the cost and lack of a chelating-group for imaging applications represent limitations overcome by **1**. Both the synthetic and conjugation chemistry described here are straightforward and can be affected with a minimum of effort. However, the extent to which these reactions proceed is dependent on the size and composition of the thiol. Tetravalent displays of large peptides have proven difficult to push to completion. Critically, conjugation can be accomplished in a range of solvents—from organic solvents to aqueous solutions—to incorporate a range of thiol-containing species. The value of this conjugation strategy—maleimide and thiol—over alternatives has been reported: Wangler *et al.* showed that thiol-maleimide couplings proceed more effectively than oxime formation or copper-catalyzed cycloadditions [26]. Finally, we note that, when the flexible dendritic domains are fully extended, **1** places ligands in the corners of a rectangular array measuring ~2.5 nm by ~4.2 nm.

Supplementary Materials: The following are available online at: <http://www.mdpi.com/1420-3049/21/3/335/s1>; ESI-TOF MS, $^1\text{H-NMR}$, $^{13}\text{C-NMR}$ and Stability test.

Acknowledgments: We thank the Robert A. Welch Foundation (P-0008), the DOD (W81XWH-12-1-0338) and the NIH (R01 CA 159144) for support.

Author Contributions: C.S.L. and E.E.S. conceived and designed the experiments; C.S.L. performed a majority of the experiments; K.J. assisted in the preparation of peptides and conjugation reactions. All contributed to the preparation of the paper.

Conflicts of Interest: The authors declare no conflict of interest.

References

- McCarthy, J.R.; Weissleder, R. Multifunctional magnetic nanoparticles for targeted imaging and therapy. *Adv. Drug Deliv. Rev.* **2008**, *60*, 1241–1251. [[CrossRef](#)] [[PubMed](#)]
- Janib, S.M.; Moses, A.S.; MacKay, J.A. Imaging and drug delivery using theranostic nanoparticles. *Adv. Drug Deliv. Rev.* **2010**, *62*, 1052–1063. [[CrossRef](#)] [[PubMed](#)]

3. Kelkar, S.S.; Reineke, T.M. Theranostics: Combining imaging and therapy. *Bioconjug. Chem.* **2011**, *22*, 1879–1903. [[CrossRef](#)] [[PubMed](#)]
4. Duncan, R.; Gaspar, R. Nanomedicine(s) under the microscope. *Mol. Pharm.* **2011**, *8*, 2101–2141. [[CrossRef](#)] [[PubMed](#)]
5. Jokerst, J.V.; Gambhir, S.S. Molecular imaging with theranostic nanoparticles. *Acc. Chem. Res.* **2011**, *44*, 1050–1060. [[CrossRef](#)] [[PubMed](#)]
6. Yu, M.K.; Park, J.; Jon, S. Targeting strategies for multifunctional nanoparticles in cancer imaging and therapy. *Theranostics* **2012**, *2*, 43–44. [[CrossRef](#)] [[PubMed](#)]
7. Lartigue, L.; Innocenti, C.; Kalavani, T.; Awwad, A.; Sanchez Duque, M.D.M.; Guari, Y.; Larionova, J.; Guerin, C.; Montero, J.-L.G.; Barragan-Montero, V.; *et al.* Water-dispersible sugar-coated iron oxide nanoparticles. An evaluation of their relaxometric and magnetic hyperthermia properties. *J. Am. Chem. Soc.* **2011**, *133*, 10459–10472. [[CrossRef](#)] [[PubMed](#)]
8. Lee, J.E.; Lee, N.; Kim, T.; Kim, J.; Hyeon, T. Multifunctional mesoporous silica nanocomposite nanoparticles for theranostic applications. *Acc. Chem. Res.* **2011**, *44*, 893–902. [[CrossRef](#)] [[PubMed](#)]
9. Cheng, S.-H.; Lee, C.-H.; Chen, M.-C.; Souris, J.S.; Tseng, F.-G.; Yang, C.-S.; Mou, C.-Y.; Chen, C.-T.; Lo, L.-W.J. Tri-functionalization of mesoporous silica nanoparticles for comprehensive cancer theranostics—the trio of imaging, targeting and therapy. *Mater. Chem.* **2010**, *20*, 6149–6157. [[CrossRef](#)]
10. Jain, T.K.; Foy, S.P.; Erokwu, B.; Dimitrijevic, S.; Flask, C.A.; Labhasetwar, V. Magnetic resonance imaging of multifunctional pluronic stabilized iron-oxide nanoparticles in tumor-bearing mice. *Biomaterials* **2009**, *30*, 6748–6756. [[CrossRef](#)] [[PubMed](#)]
11. Moon, G.D.; Choi, S.-W.; Cai, X.; Li, W.; Cho, E.C.; Jeong, U.; Wang, L.V.; Xia, Y. A new theranostic system based on gold nanocages and phase-change materials with unique features for photoacoustic imaging and controlled release. *J. Am. Chem. Soc.* **2011**, *133*, 4762–4765. [[CrossRef](#)] [[PubMed](#)]
12. Ho, Y.-P.; Leong, K.W. Quantum dot-based theranostics. *Nanoscale* **2010**, *2*, 60–68. [[CrossRef](#)] [[PubMed](#)]
13. Ke, H.; Wang, J.; Dai, Z.; Jin, Y.; Qu, E.; Xing, Z.; Guo, C.; Yue, X.; Liu, J. Gold-nanoshelled microcapsules: A theranostic agent for ultrasound contrast imaging and photothermal therapy. *Angew. Chem. Int. Ed. Eng.* **2011**, *50*, 3017–3021. [[CrossRef](#)] [[PubMed](#)]
14. Yang, K.; Feng, L.; Shi, X.; Liu, Z. Nano-graphene in biomedicine: Theranostic applications. *Chem. Soc. Rev.* **2013**, *42*, 530–547. [[CrossRef](#)] [[PubMed](#)]
15. Al-Jamal, W.T.; Al-Jamal, K.T.; Bomans, P.H.; Frederik, P.M.; Kostarelos, K. Functionalized-quantum-dot-liposome hybrids as multimodal nanoparticles for cancer. *Small* **2008**, *4*, 1406–1415. [[CrossRef](#)] [[PubMed](#)]
16. Al-Jamal, W.T.; Kostarelos, K. Liposomes: From a clinically established drug delivery system to a nanoparticle platform for theranostic nanomedicine. *Acc. Chem. Res.* **2011**, *44*, 1094–1104. [[CrossRef](#)] [[PubMed](#)]
17. Li, X.; Qian, Y.; Liu, T.; Hu, X.; Zhang, G.; You, Y.; Liu, S. Amphiphilic multiarm star block copolymer-based multifunctional unimolecular micelles for cancer targeted drug delivery and magnetic resonance imaging. *Biomaterials* **2011**, *32*, 6595–6805. [[CrossRef](#)] [[PubMed](#)]
18. Shi, J.; Xiao, Z.; Kamaly, N.; Farokhzad, O.C. Self-assembled targeted nanoparticles: Evolution of technologies and bench to bedside translation. *Acc. Chem. Res.* **2011**, *44*, 1123–1134. [[CrossRef](#)] [[PubMed](#)]
19. Shukla, R.; Thomas, T.P.; Peters, J.; Kotlyar, A.; Myc, A.; Bakers, J.R., Jr. Tumor angiogenic vasculature targeting with PAMAM dendrimer-RGD conjugates. *Chem. Comm.* **2005**, 5739–5741. [[CrossRef](#)] [[PubMed](#)]
20. Li, Y.; He, H.; Jia, X.; Lu, W.-L.; Lou, J.; Wei, Y. A dual-targeting nanocarrier based on poly(amidoamine) dendrimers conjugated with transferrin and tamoxifen for treating brain gliomas. *Biomaterials* **2012**, *33*, 3899–3908. [[CrossRef](#)] [[PubMed](#)]
21. Tomalia, D.A. In quest of a systematic framework for unifying and defining nanoscience. *J. Nanopart. Res.* **2009**, *11*, 1251–1310. [[CrossRef](#)] [[PubMed](#)]
22. Tomalia, D.A.; Khanna, S.N. A systematic framework and nanoperic concept for unifying nanoscience: Hard/Soft nanoelements, superatoms, meta-atoms, new emerging properties, periodic property patterns, and predictive mendeleev-like nanoperic tables. *Chem. Rev.* **2016**, *116*, 2705–2774. [[CrossRef](#)] [[PubMed](#)]
23. Kannan, R.M.; Nance, E.; Kannan, S.; Tomalia, D.A. Emerging concepts in dendrimer-based nanomedicine: From design principles to clinical applications. *J. Internal Med.* **2014**, *276*, 579–617. [[CrossRef](#)] [[PubMed](#)]
24. Enciso, A.E.; Abid, Z.M.; Simanek, E.E. Rapid, semi-automated convergent synthesis of low generation triazine dendrimers using microwave assisted reactions. *Polym. Chem.* **2014**, *5*, 4635–4640. [[CrossRef](#)]

25. Gray, W.D.; Wu, R.J.; Yin, X.; Zhou, J.; Davis, M.E.; Luo, Y. Dendrimeric bowties featuring hemispheric-selective decoration of ligands for microRNA-based therapy. *Biomacromolecules* **2013**, *14*, 101–109. [[CrossRef](#)] [[PubMed](#)]
26. Wängler, C.; Mashauer, S.; Prante, O.; Schafer, M.; Schmirrmacher, R.; Bartenstein, P.; Eisenhut, M.; Wängler, B. Multimerization of cRGD peptides by click chemistry: Synthetic strategies, chemical limitations, and influence on biological properties. *ChemBioChem* **2010**, *11*, 2168–2181. [[CrossRef](#)] [[PubMed](#)]

Sample Availability: Samples of the compounds are available from the authors.



© 2016 by the authors; licensee MDPI, Basel, Switzerland. This article is an open access article distributed under the terms and conditions of the Creative Commons by Attribution (CC-BY) license (<http://creativecommons.org/licenses/by/4.0/>).